Chapter 4

Experimental result and discussion

4.1 Raw material characterization

4.1.1 Particle size determination

Particle size distribution was measured by laser scattering particle size analyzer. Table 4.1 shows the average particle size and standard deviation of each raw material used for the experiment.

Table 4.1 Average particle size and standard deviation of raw materials

Raw materials	Average particle size(μm)	S.D.(μm)
Alumina A-21	0.95	1.06
Aluminium oxide from waste Al-coating	1.21	2.35
Aluminium oxide from MTEC	1.15	2.88
SiO_2-H	10.14	6.92
SiO_2-N	8.40	5.90

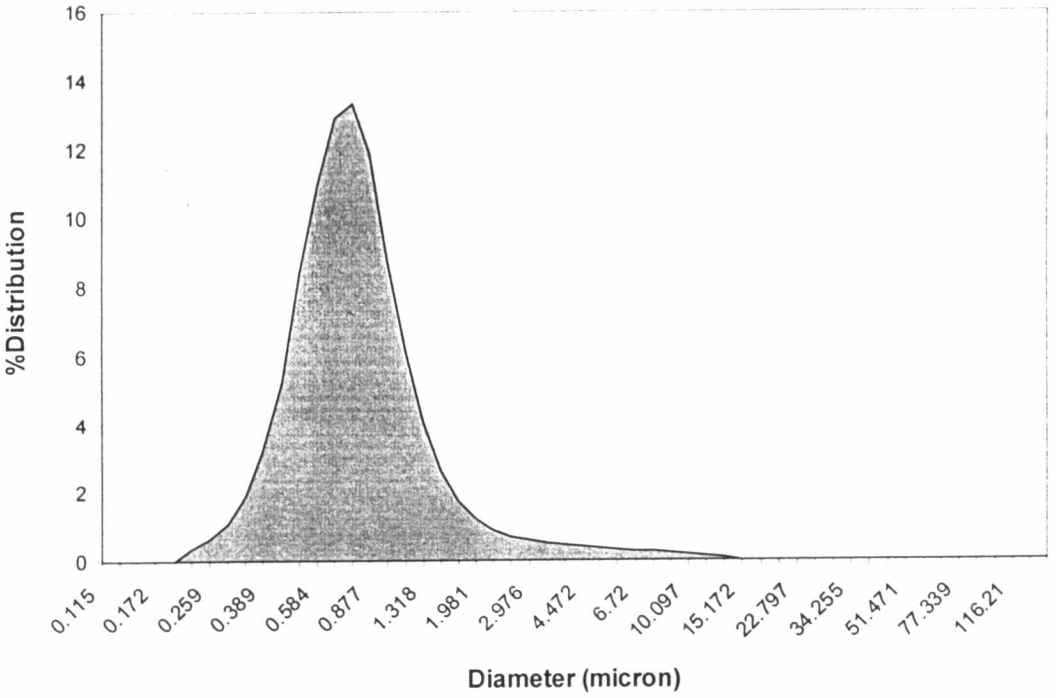

Fig.4.1 Particle size distribution of alumina A-21 grinding for 11 h.

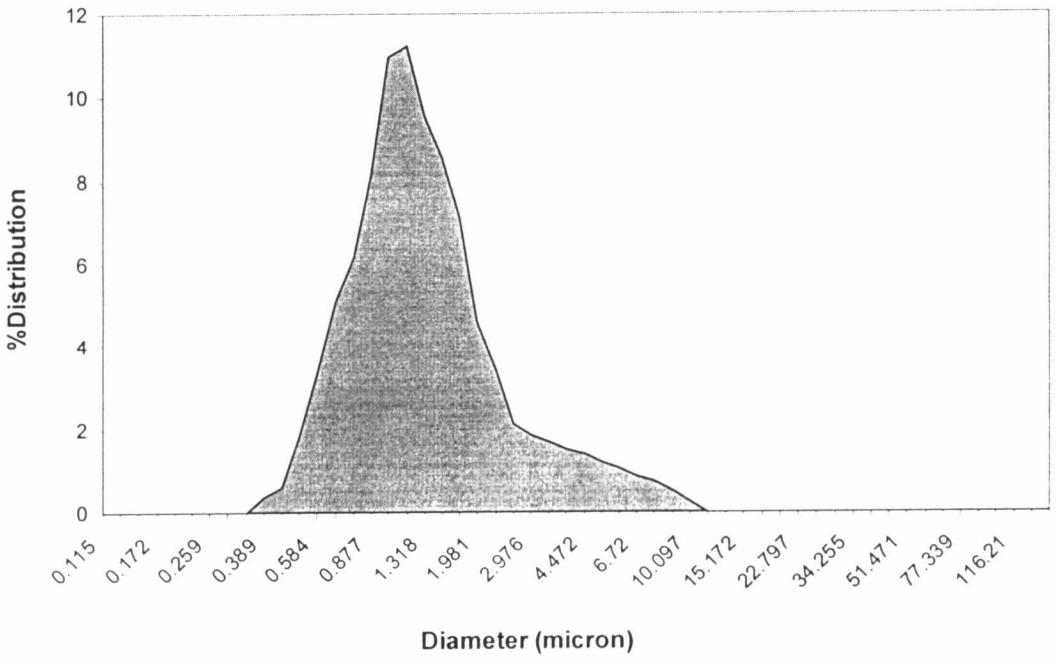

Fig.4.2 Particle size distribution of aluminium oxide from waste Al grinding for 4 h.

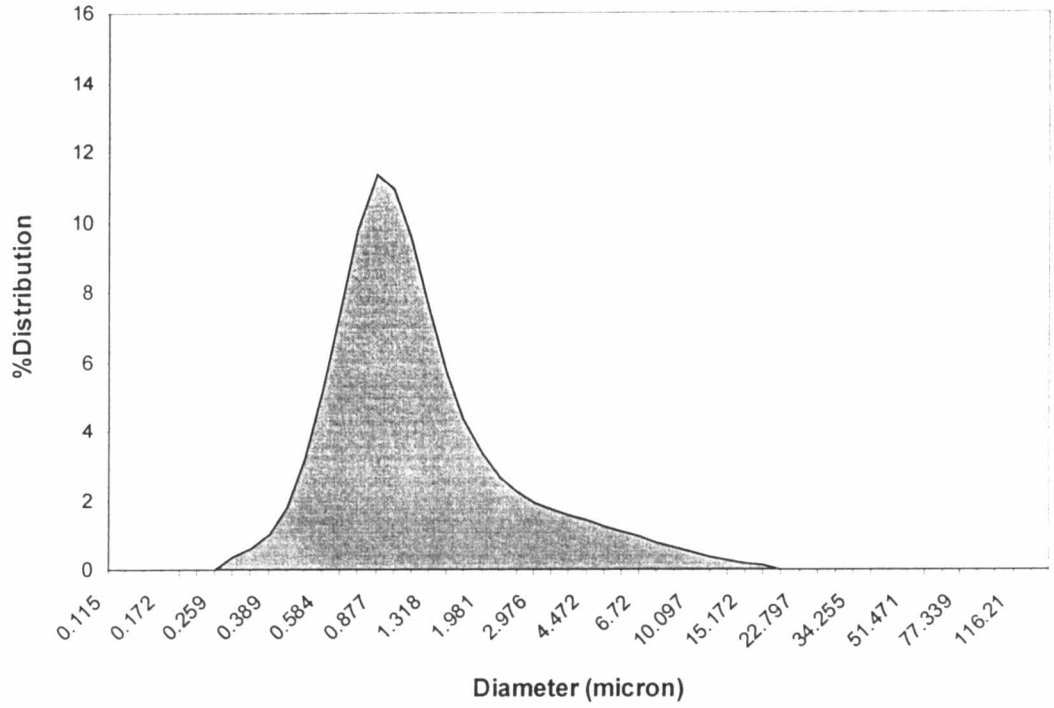

Fig.4.3 Particle size distribution of aluminium oxide from MTEC grinding for 4 h.

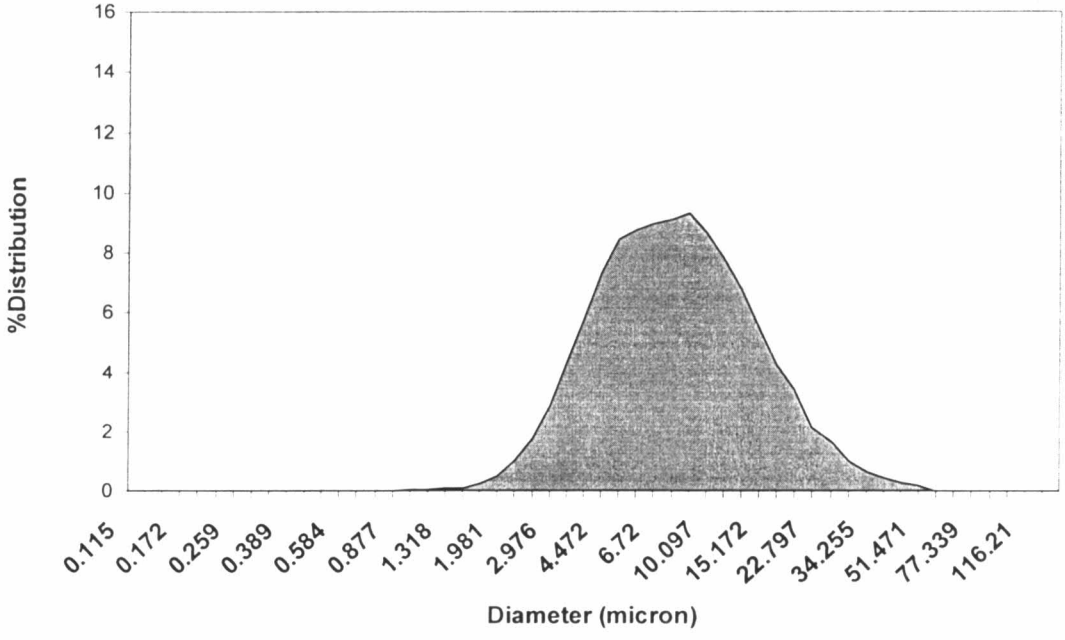

Fig.4.4 Particle size distribution of SiO_2-H (no grinding).

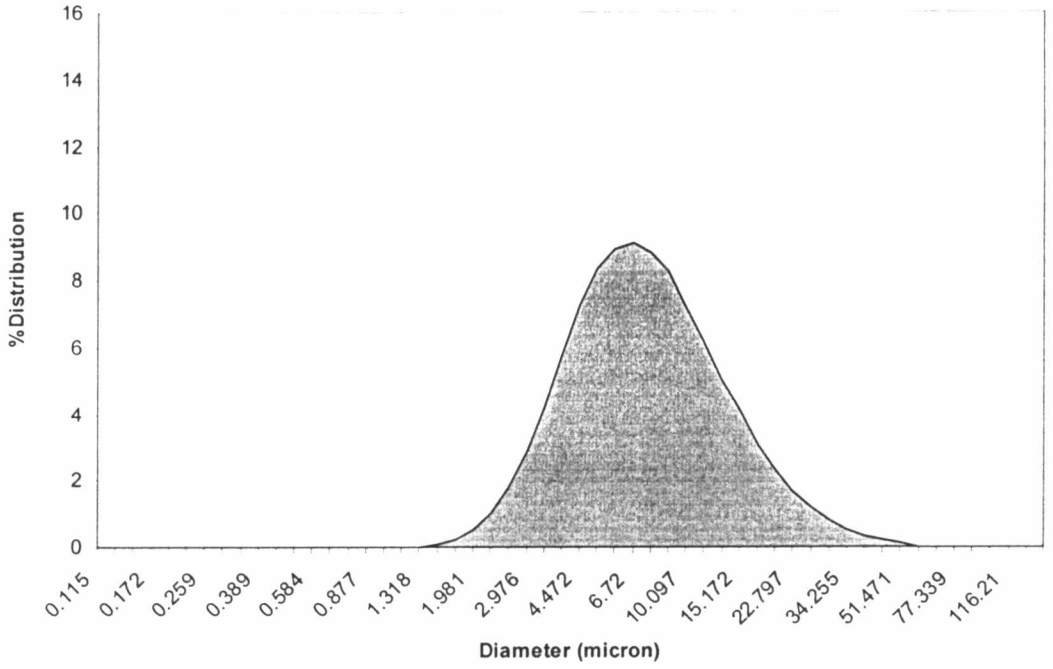

Fig.4.5 Particle size distribution of SiO_2-N (no grinding).

From Table 4.1 and Fig. 4.1-4.5, the average particle size of alumina A-21 is smaller than that of aluminium oxide from waste and from MTEC, but A-21 must be ground longer than the others. Comparing the average particle size of two kinds of silica, SiO_2-N is smaller than SiO_2-H.

In fact, particle sizes of silica from rice husk are less than 100 nm (detected by transmittion electron microscope), however, the small particle of silica agglomerated into granules. That is why average particle sizes are so large when detected by laser scattering analyzer.

4.1.2 Specific surface area

Specific surface areas of raw materials are shown in table 4.2

Table 4.2 Specific surface area of raw materials

Raw materials	Specific surface area (m^2/g)
Alumina A-21	19
Aluminium oxide from calcined waste	136
Aluminium oxide from MTEC	105
Waste from Al-coating(consisting mainly of gibbsite)	9
SiO_2-N	291
SiO_2-U	23
SiO_2-H	182

From the data shown in Table 4.1 and Table 4.2, particle size and specific surface area are not related. The smaller size of A-21 does not show high specific surface area when compare with aluminium oxide from MTEC and Aluminium oxide from waste Al-coating.

Silica powders from the proprietary method gained higher specific surface area than the silica treated by acid.

4.1.3 Phase analysis of raw materials by XRD

XRD patterns of Al_2O_3 and SiO_2 are shown in Fig.4.6 and Fig.4.7

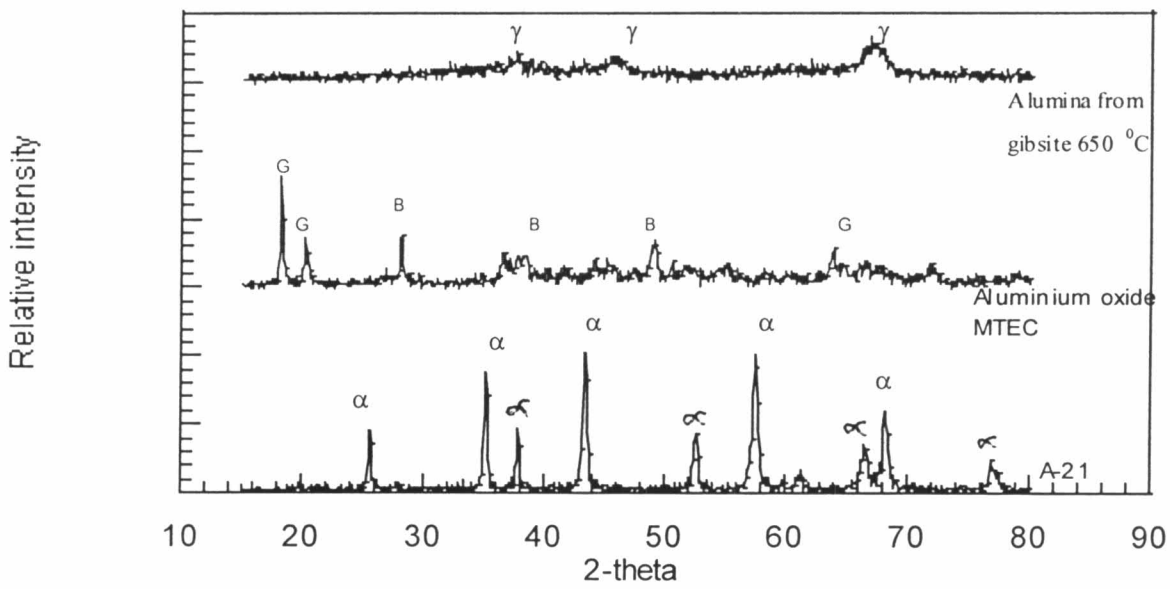

α- Alpha alumina, γ- Gamma alumina, G- Gibbsite, B- Boehmite

Fig.4.6 XRD patterns of 3 kinds of aluminium oxide.

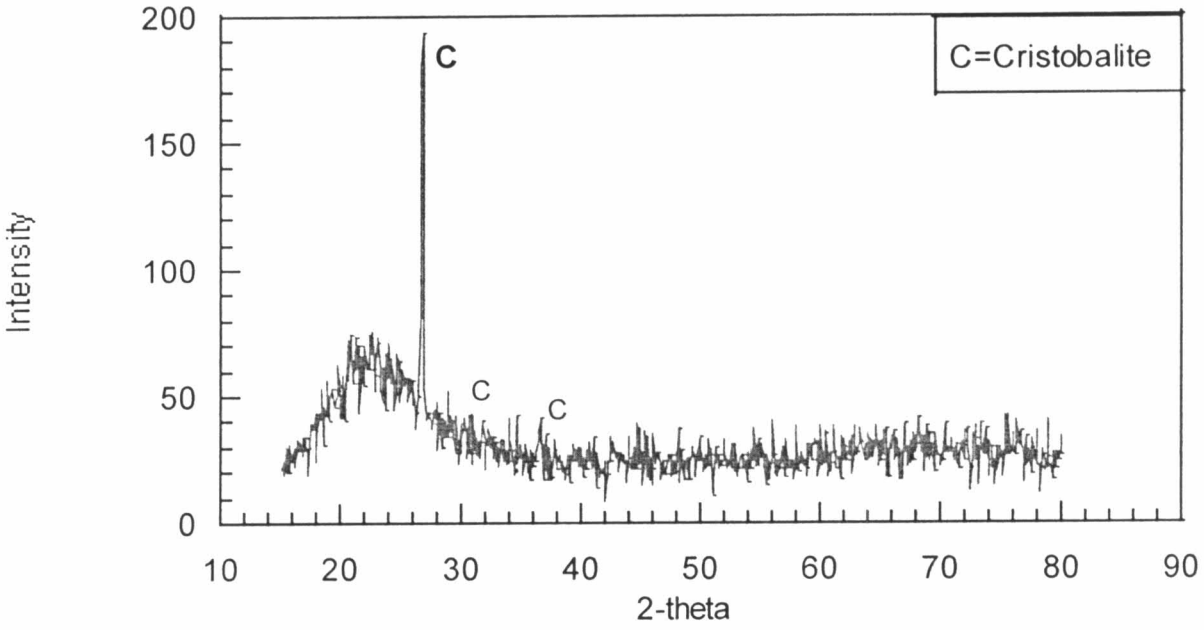

Fig.4.7 XRD pattern of SiO_2-H.

From Fig.4.6 aluminium oxide which is calcined from waste Al-coating at temperature of 650°C is amorphous phase, aluminium oxide from MTEC includes some amount of boehmite and gibbsite and alumina A-21 is completely α-Al_2O_3. Fig.4.7 shows XRD-pattern of SiO_2-H. SiO2-H is composed of cristobalite and amorphous phase.

4.1.4 Composition of starting materials analyzed by X-Ray Fluorescence

Starting materials for this experiment were analyzed by XRF in order to examine %SiO_2 and %Al_2O_3 which are main oxides in mullite and also %impurities such as alkali oxide, Fe_2O_3 etc. Oxide contents of starting materials are shown in table 4.3

Table 4.3 Oxide contents of starting materials analyzed by X-ray fluorescence.

%Oxide	SiO_2-H	SiO_2-N	SiO_2-U	Al_2O_3 A-21	Aluminium oxide MTEC	Aluminium oxide from calcined waste	Waste from Al-coating
Al_2O_3	0.80	0.91	1.12	99.60	98.78	92.89	90.78
SiO_2	99.06	98.10	97.36	0.01	0.36	1.26	1.28
Fe_2O_3	0.01	0.00	0.00	0.01	0.04	0.26	0.44
Na_2O	0.00	0.04	0.01	0.25	0.44	1.99	3.23
CaO	0.06	0.83	1.01	-	0.00	0.14	0.34
K_2O	0.03	0.07	0.33	-	0.00	0.03	0.21
MgO	0.00	0.03	0.05	-	0.39	0.77	0.98
TiO_2	0.00	0.00	0.00	-	0.00	0.22	0.25
MnO_2	0.02	0.02	0.02	-	0.00	0.34	0.36
CuO	0.00	0.00	0.00	-	0.00	0.85	0.87
NiO	0.00	0.00	0.00	-	0.00	1.10	1.16
Cr_2O_3	0.00	0.00	0.01	-	0.00	0.05	0.03
ZnO	0.00	0.00	0.00	-	0.00	0.09	0.07
PbO	0.00	0.00	0.00	-	0.00	0.00	0.00

4.2 Characterization of sintered specimens

4.2.1 Shrinkage

The relationship between pressing pressure and shrinkage of specimens formula 1 is shown in Fig. 4.8.

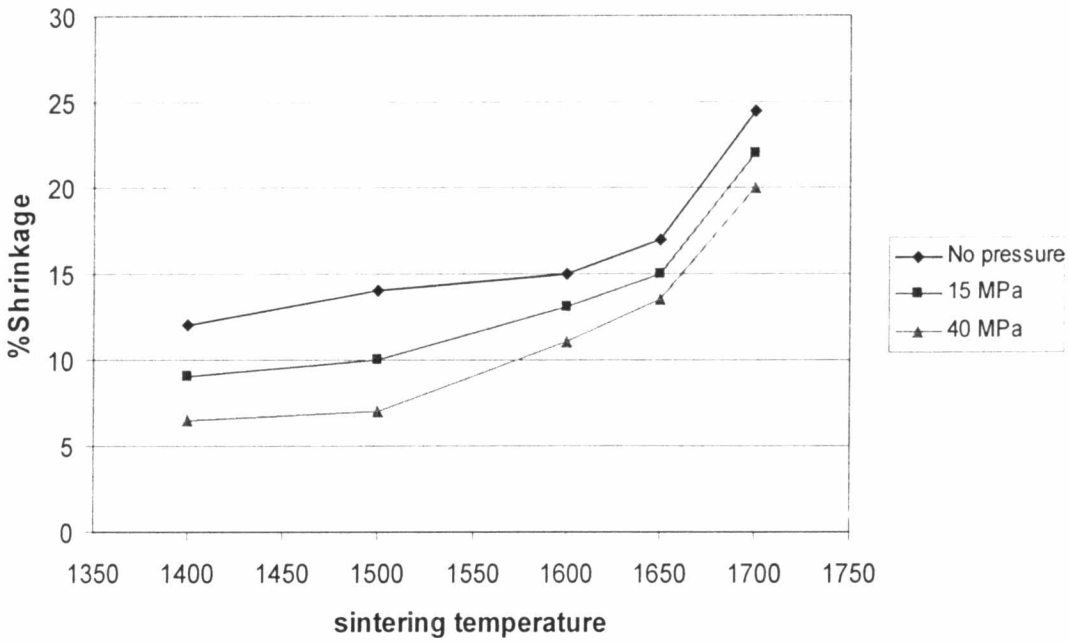

Fig.4.8 Relationship between shrinkage and sintering temperature of specimens Formula 1 at various pressing pressures.

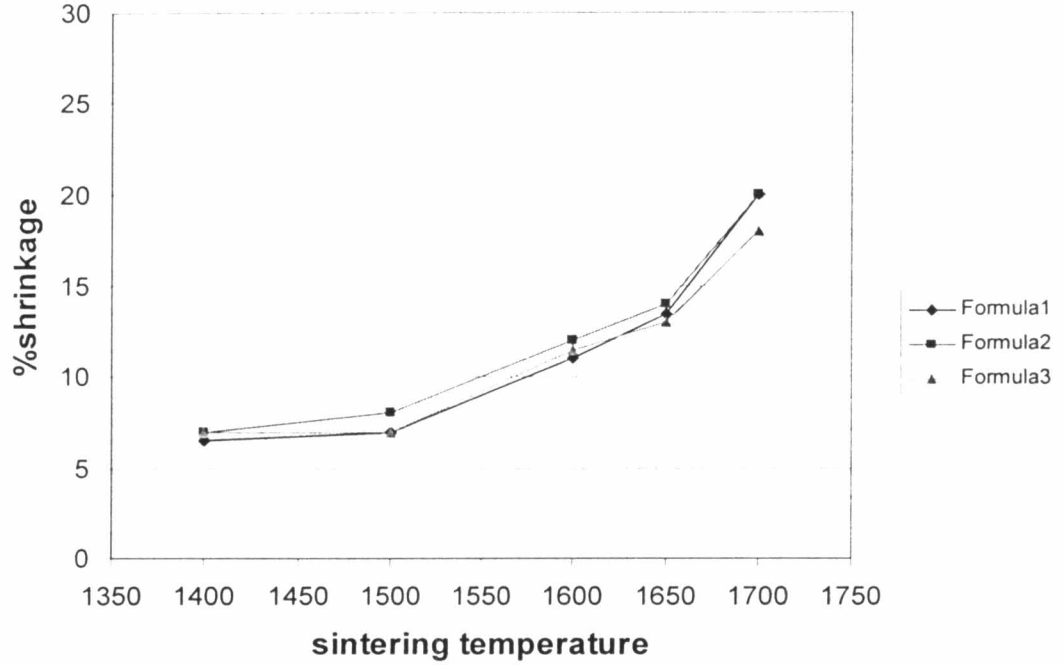

Fig.4.9 Relationship between shrinkage and sintering temperature at different ratios of alumina and silica.

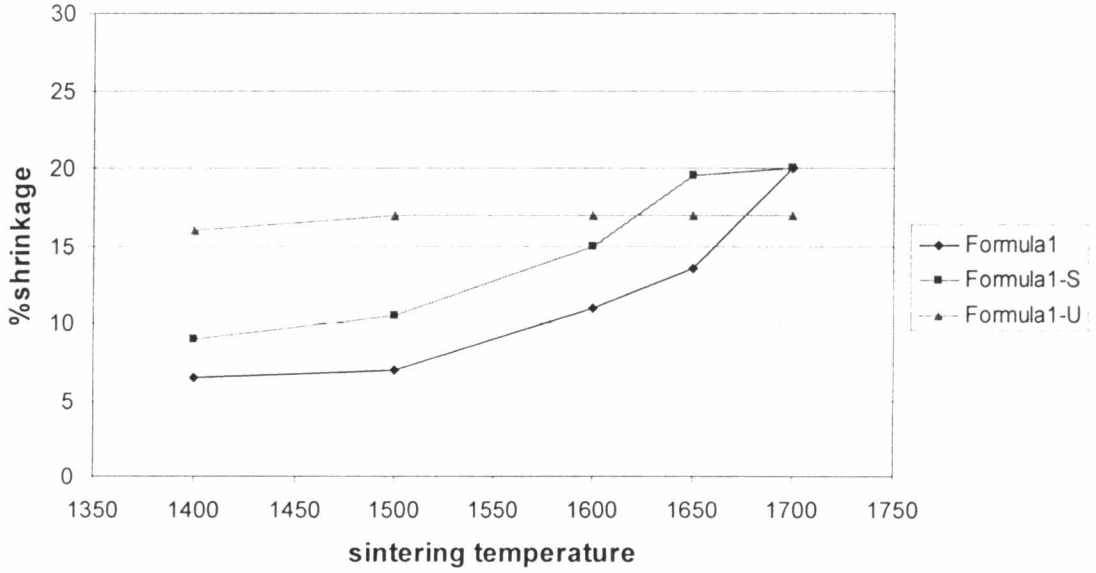

Fig. 4.10 Relationship between shrinkage and sintering temperature of different silica powders (same alumina A-21).

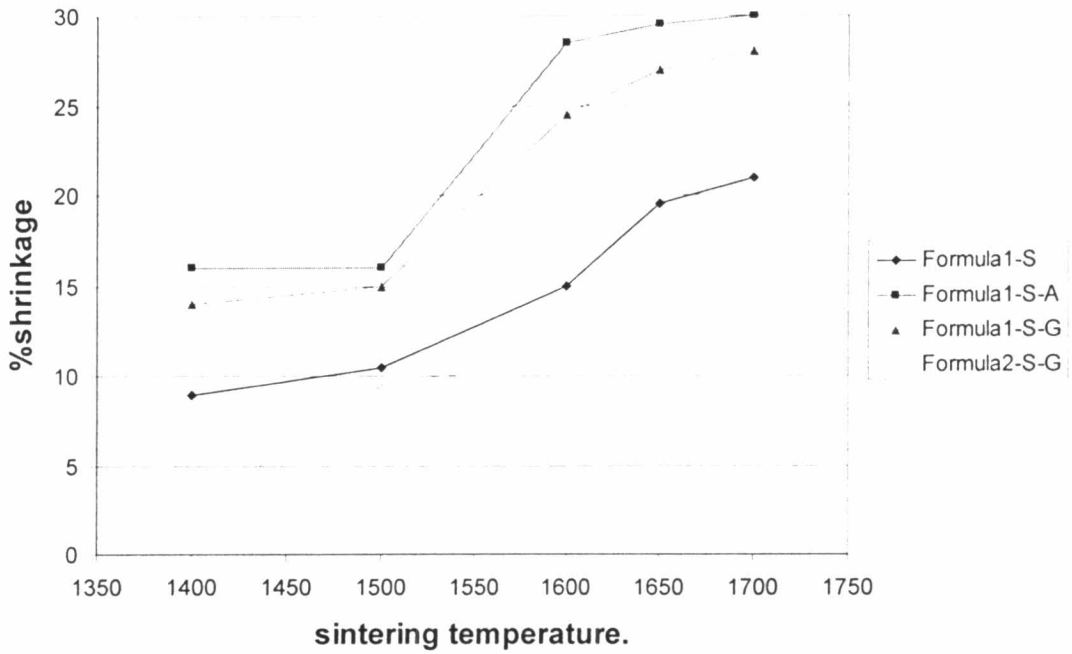

Fig.4.11 Relationship between shrinkage and sintering temperature of alumina from different sources (same SiO_2-N).

In Fig.4.8 at each temperature, when pressing pressure for forming the specimen increases, shrinkage decreases and difference in shrinkage value between the specimen pressed with no pressure and with 40 MPa pressure was about 5% at each temperature. Then if we increase the pressure for forming, we can reduce the shrinkage.

Fig. 4.9 shows that high Al_2O_3:SiO_2 ratio (Table 3.2. Formula 3, excess Al_2O_3), lowers the shrinkage of the specimen than others at 1700 °C because it did not sinter to higher density as shown in Fig.4.13.

Fig.4.10, 4.11 and Appendix 7 show %shrinkage of each formula. Formula1-A and 1-S-A which contain aluminium oxide from MTEC show higher shrinkage than the others even with different silica powders because the aluminium oxide from MTEC has more impurities (from Table 4.3) and higher specific surface area (Table 4.2) than alumina A-21. Moreover, aluminium oxide from MTEC is a mixture of boehmite and gibbsite as

shown in Fig.4.6. It is almost amorphous when examined by XRD then it shrinks more than A-21.

Formula 1-S-G, containing alumina from waste Al-coating, shows lower shrinkage than aluminium oxide from MTEC but still high when compared with A-21 and waste from Al-coating. This may come from impurities in alumina that induce glassy phase between boundaries of mullite grains.

Formula 2-S-G, using waste from Al-coating, shows the lowest shrinkage (at 1700 °C only 13 %) because waste from Al-coating has low specific gravity and high loss on ignition, so specimen containing waste from Al-coating can be used to produce a porous material for another application, i.e. , thermal insulator, hot filter etc.

4.2.2 Bulk density and relative density.

Densities of sintered specimens were measured by Archimedes' method and then compared with calculated theoretical density of the corresponding formula. All data are shown in Appendix1. The relationship between relative density and sintering temperature of formula 1 (stoichiometric formula) at various pressing pressures is shown in Fig.4.12

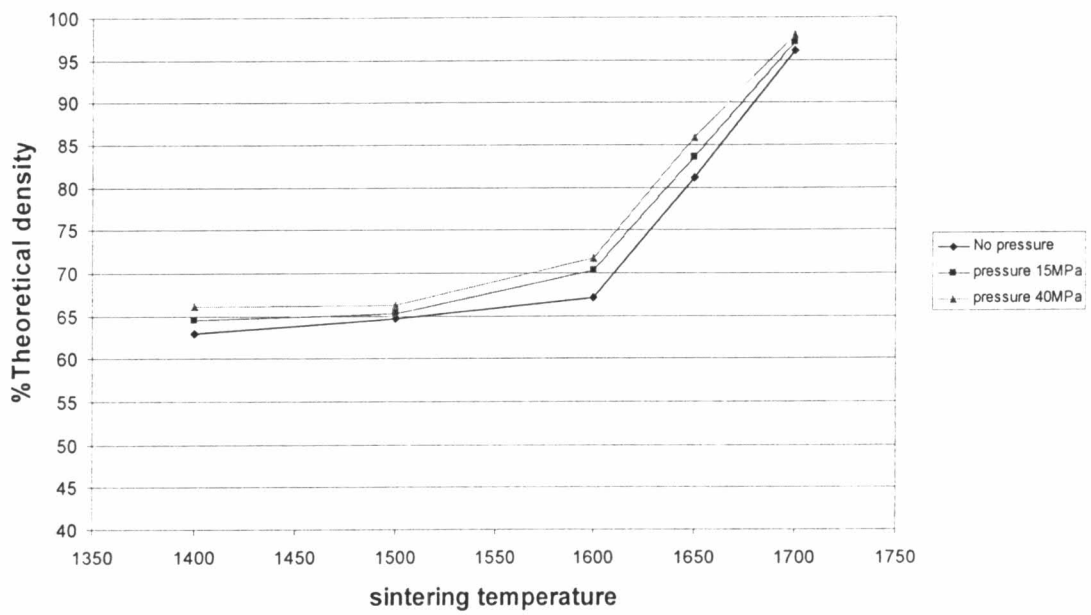

Fig.4.12 Relationship between relative density and sintering temperature at various pressing pressures for Formula1.

When pressing pressure is increased, the relative densities of the specimens increase because high pressure can produce a good compaction of the specimens.

The relationship between relative densities of specimens with various percentages of alumina and silica and sintering temperatures is shown in figure.4.13

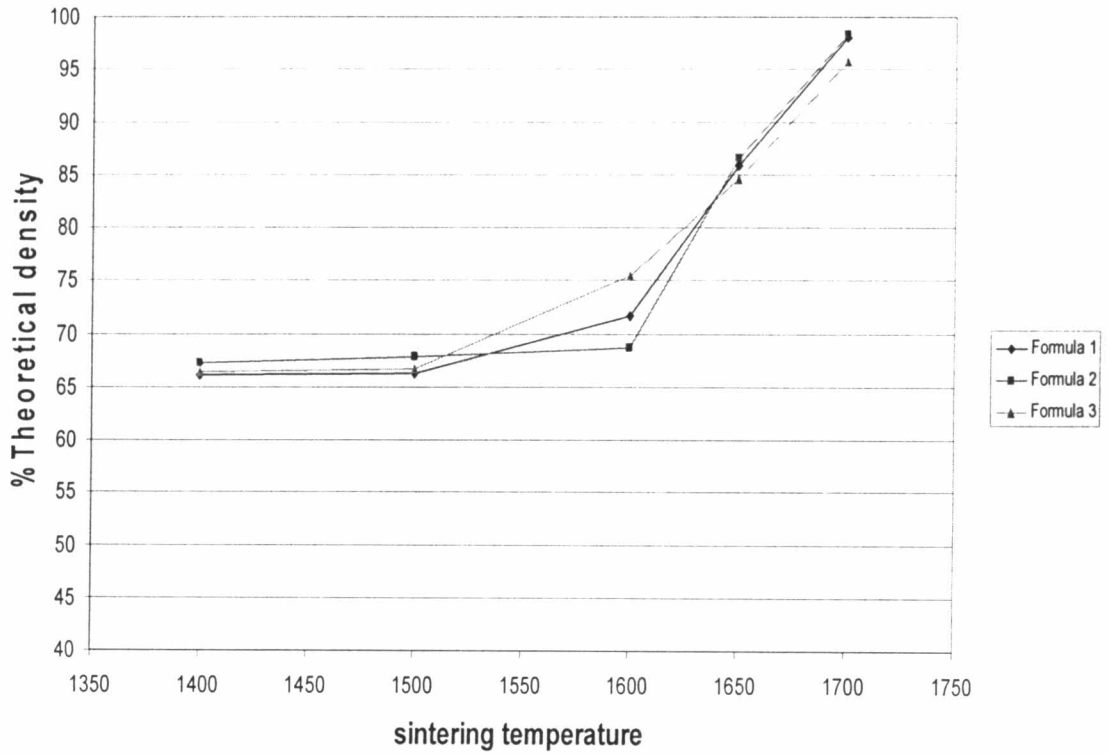

Fig.4.13 Relationship between relative density and sintering temperature of specimens with various ratios of Al_2O_3:SiO_2

As shown in Fig. 4.13, Formula 1 and 2 can reach to full density at 1700 °C but Formula 3 is only about 95 % of theoretical density. It means that we can sinter dense mullite when using stoichiometric formula or excess silica in a mixture.

For other formulas shown in Table 3.2, the relationship between relative density and sintering temperature is shown in Fig.4.14, Fig 4.15 and Appendix 7.

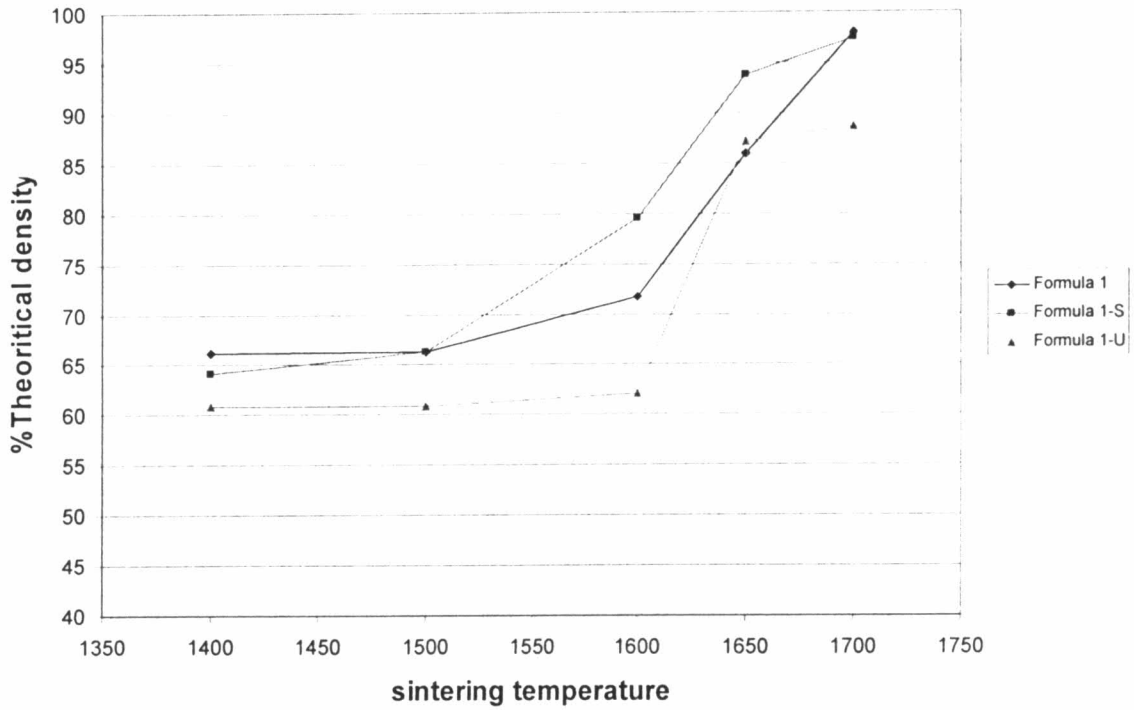

Fig.4.14 Relationship between relative density and sintering temperature of specimens containing different silica powders (same alumina A-21)

Formula 1 and 1-S which contains alumina A-21 reach almost full density at 1700 °C due to the purity of alumina A-21. Alumina and silica react completely to form mullite, hence, less glassy phase forms between grains. Formula 1-U contains alumina A-21 and untreated silica which is low specific surface area. The low silica content and high impurties such as alkali oxide cause glassy phase which results in low density (only 89% at 1700 °C).

The reason why the relative densities of specimens derived from aluminium oxide from MTEC and alumina from waste Al-coating are higher than the specimens containing A-21 at 1600 °C may be due to the impurities in the aluminium oxides such as alkali oxide. Such oxides can cause the formation of glassy phase between grain boundaries of mullite, and also reside at the triple points. Therefore the sintered mullite is unable to attain much higher density at 1700°C.

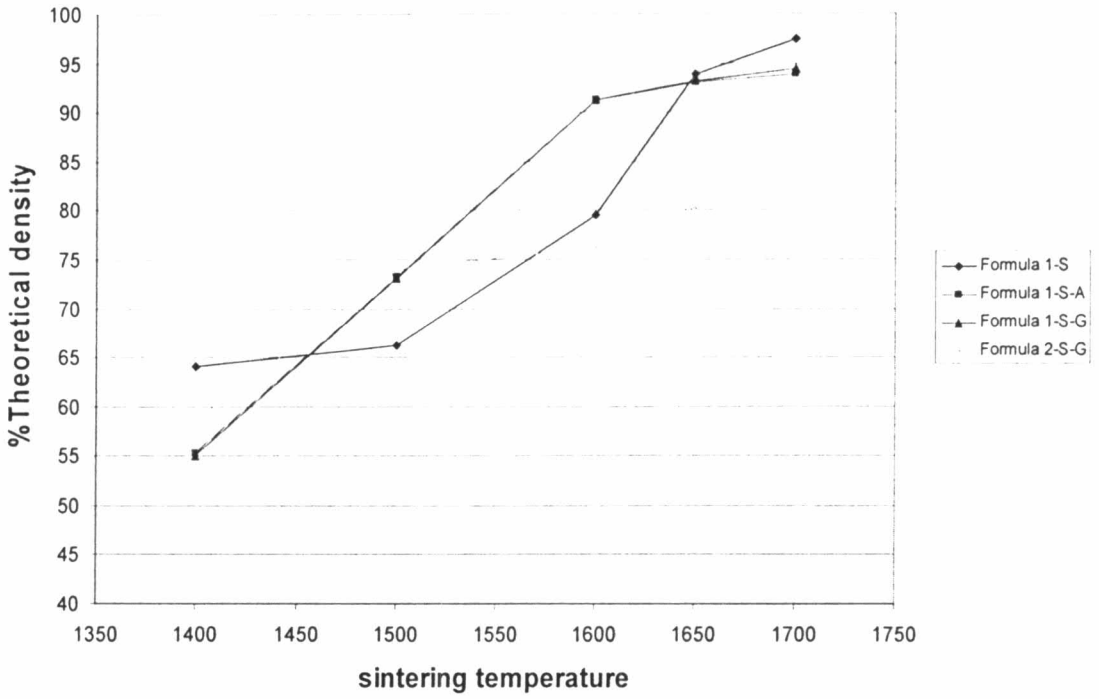

Fig.4.15 Relationship between relative density and sintering temperature of the formula with different starting materials of alumina (same SiO_2-N)

The effect of the different alumina in the starting materials is shown in Fig. 4.15. The different starting materials give different results, Alumina A-21 shows the highest density, Aluminium oxide from MTEC and aluminium oxide from waste Al-coating give the same result and waste from Al-coating shows the lowest one, hence it is understood that waste from Al-coating is not suitable to produce a dense mullite.

4.2.3 Water absorption

Figure.4.16-4.19 show the relationship between water absorption and sintering temperature

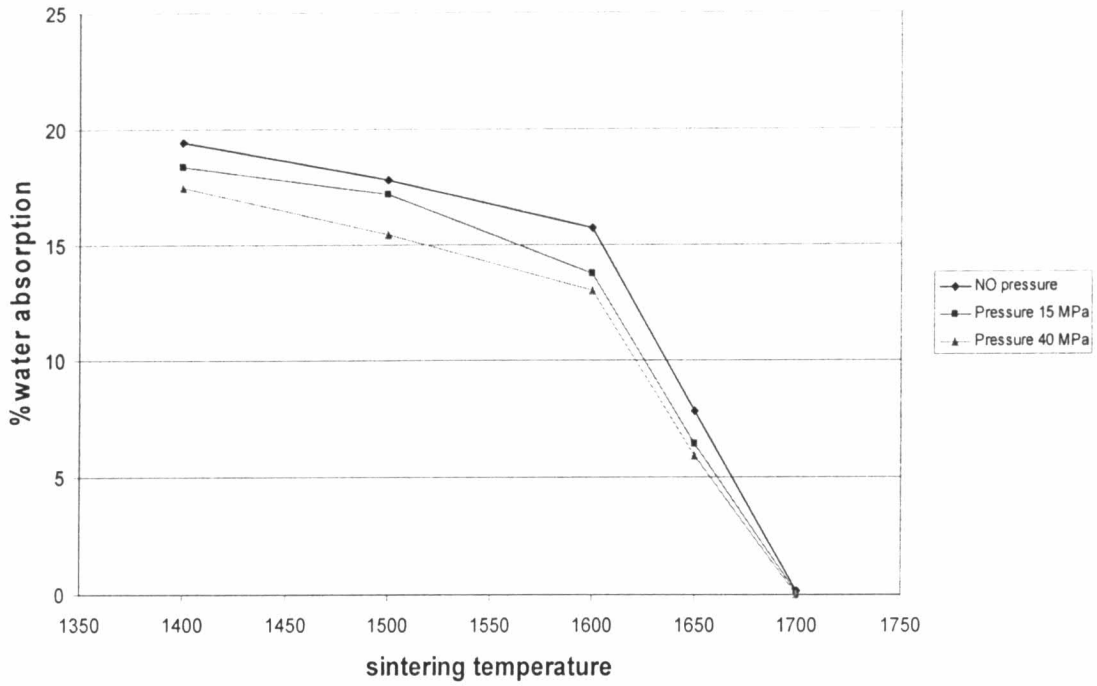

Fig.4.16 Relationship between water absorption and sintering temperature for Formula1 at various pressing pressures.

At 1400-1600 °C the specimens with no pressing pressure have higher water absorption than the specimens pressed at 15 and 40 MPa pressure, and the absorption is extremely reduced to nearly zero at 1700 °C.

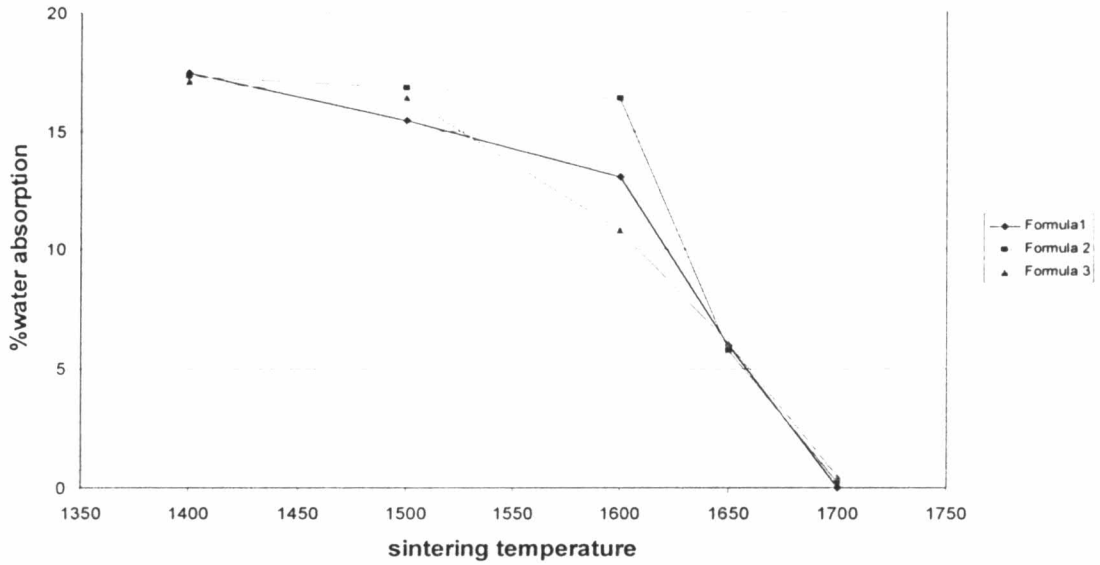

Fig.4.17 Relationship between water absorption and sintering temperature at various ratios of Al_2O_3:SiO_2(at pressing pressure of 40 MP)

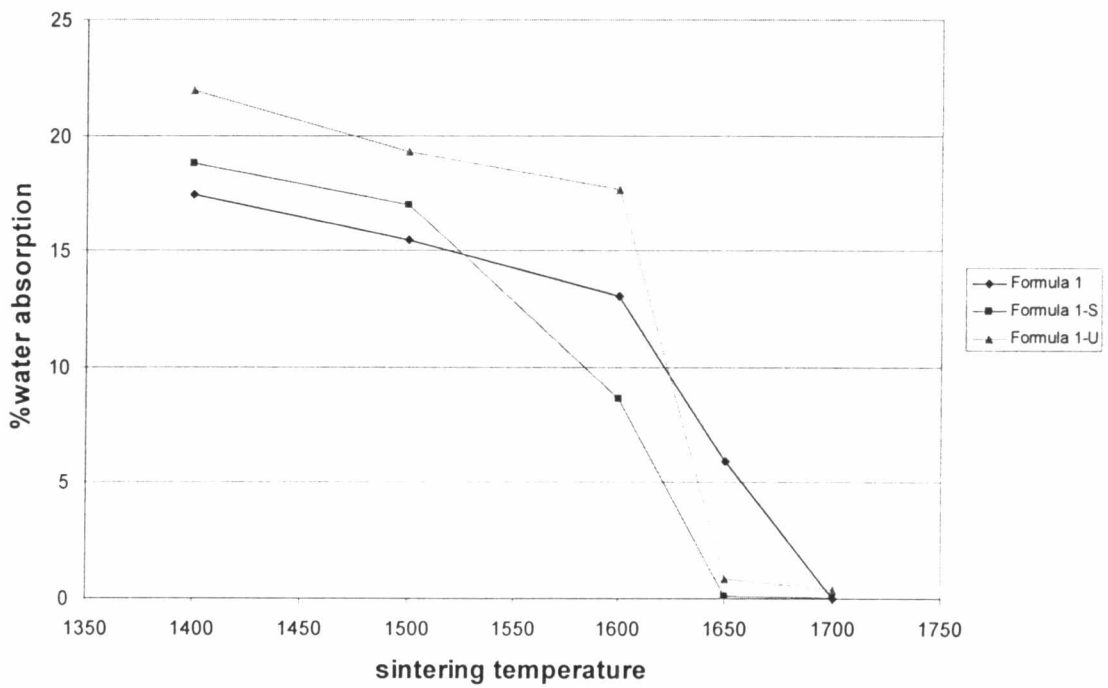

Fig.4.18 Relationship between water absorption and sintering temperature of different silica powders (same alumina A-21)

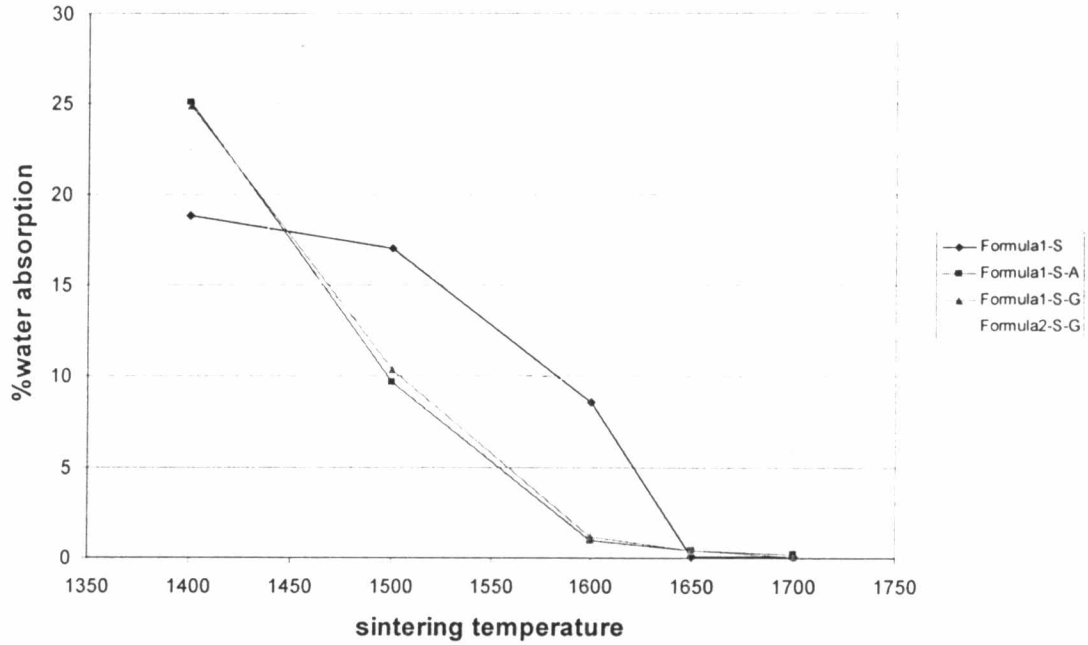

Fig.4.19 Relationship between water absorption and sintering temperature of formulas with different starting materials of alumina (same SiO_2-N)

Fig. 4.17 shows that the water absorption of Formula 2 (excess silica) has not change much at 1400-1600 °C but dramatically decreases at over 1600 °C and is almost zero at 1700 °C. Fig.4.18 and 4.19 show graph of water absorption of each formula. All of specimen have the same tendency when temperature is increased and closely to obtain zero water absorption at 1700 °C except Formula 2-S-G, which was derived from waste Al-coating (about 6%)

4.2.4 Phase analysis by X-Ray diffraction.

4.2.4.1 The effect of sintering temperature and soaking time on phase transformation of mullite

Crystal phases of sintered mullite were analyzed by X-Ray diffractometer in order to know the reaction at different sintering temperatures of each formula and starting material. The relationship between sintering temperature and crystal phases Formula 1 is shown in Fig. 4.20.

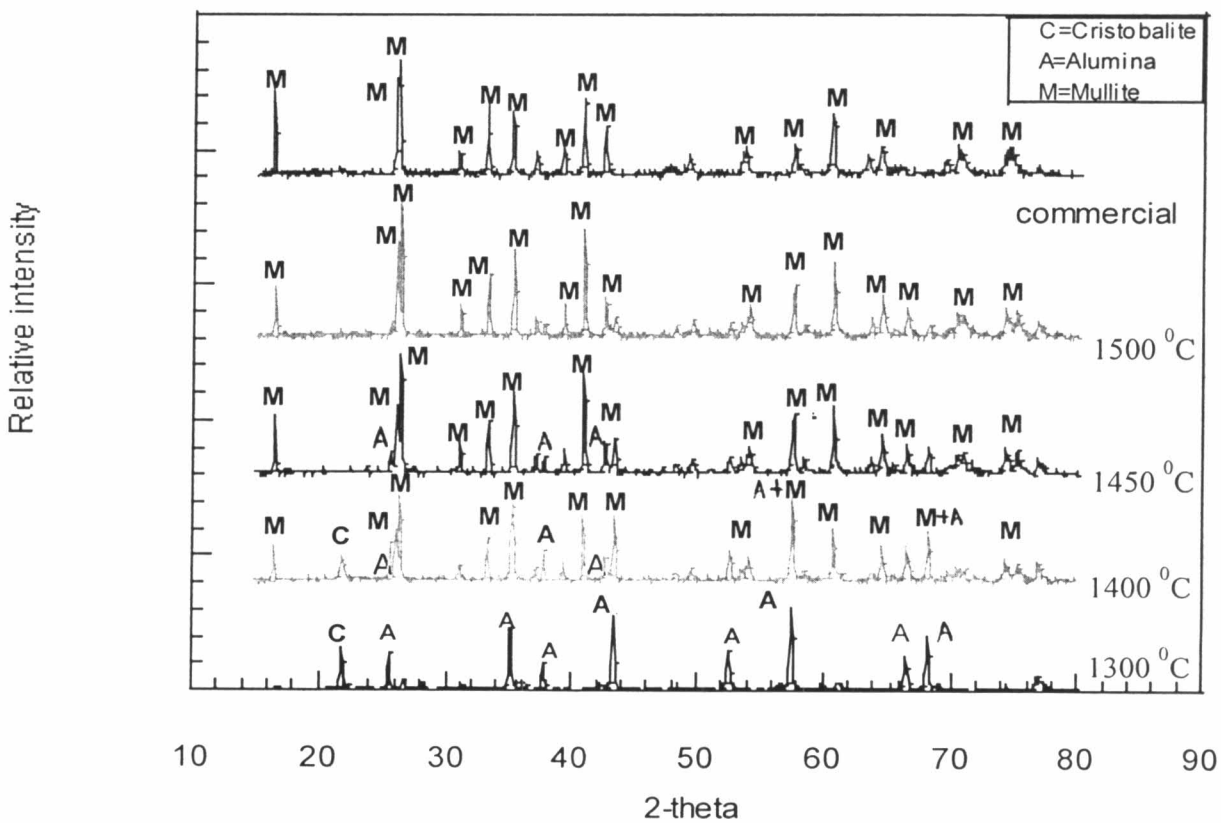

Fig 4.20 Relationship between sintering temperature and phase transformation of mullite, soaking time 5 h (Formula 1)

At 1300 °C, the specimen is composed of cristobalite, alumina and some mullite phase. When sintering temperature is increased to 1400 °C, mullite phase increases and alumina nearly disappears, while cristobalite still remains at this temperature. At 1450 °C, the whole specimen changes to mullite phase. When compared with commercial mullite powder from Japan, our synthesized mullite shows identical XRD pattern at 1450 °C.

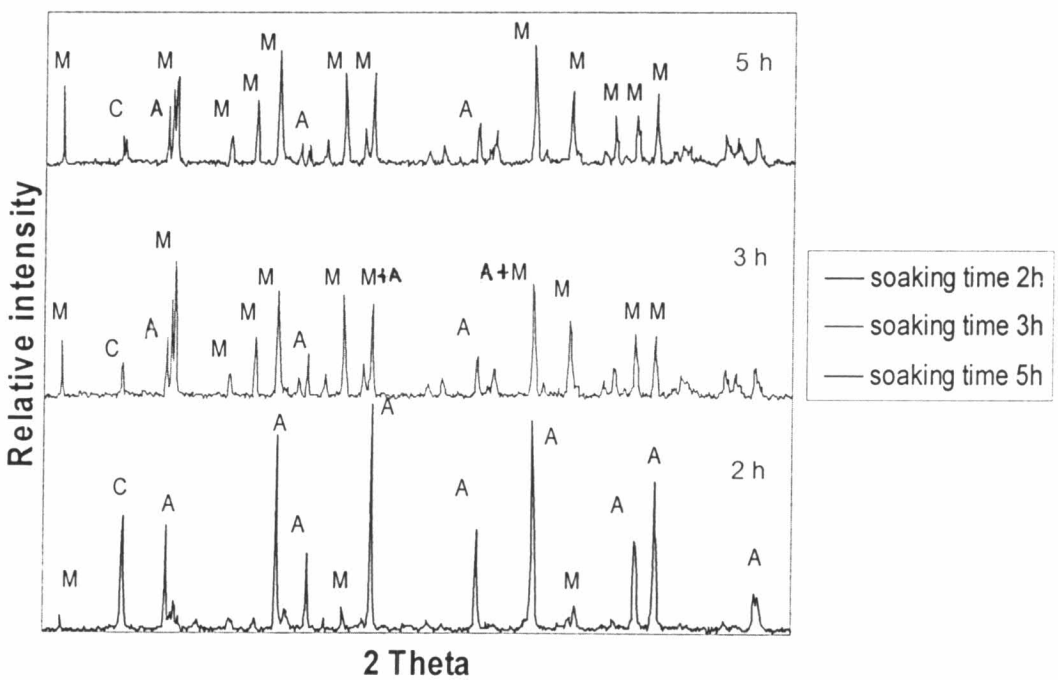

Fig.4.21 XRD patterns of the specimens at various soaking times at 1400 °C (Formula 1)

As shown in Fig.4.21, XRD pattern of the specimen which is fired at 1400 °C with a soaking time of 2h shows alumina and cristobalite peaks, and mullite phase just starts to form.

When soaking time increases, the alumina and cristobalite decrease and change to mullite phase.

From Fig. 4.20 and Fig. 4.21, the formation of mullite from the mixture between alumina and silica is affected by temperature and time, however, the temperature effect is dominant than soaking time as shown in Fig.4.22.

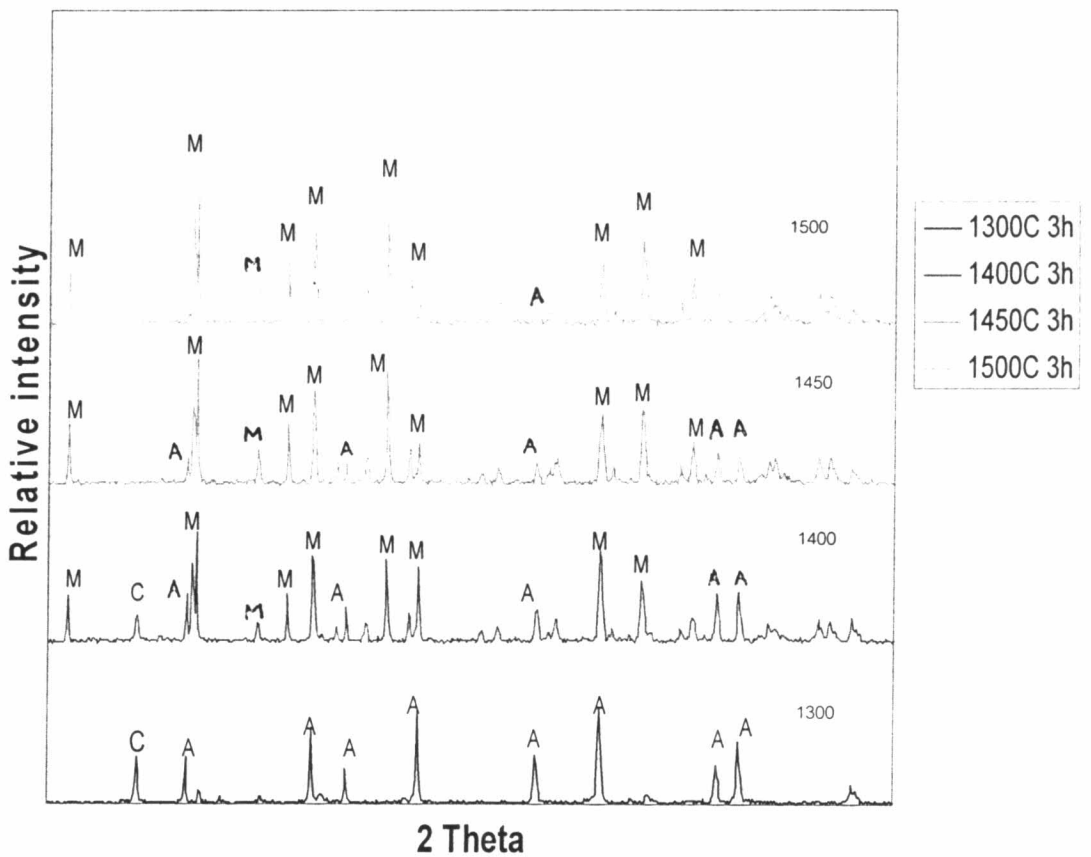

Fig.4.22 XRD patterns of the specimens at various sintering temperatures, soaking time 3 h. (Formula 1)

From Fig. 4.21 and 4.22 the mullitization can occur at low soaking time, but the content increases a little with sintering temperature. At 1450 °C for 3 h, the powder becomes fully mullitised hence cristobalite and alumina peaks totally disappear.

4.2.4.2 The effect of the starting materials for phase transformation of mullite

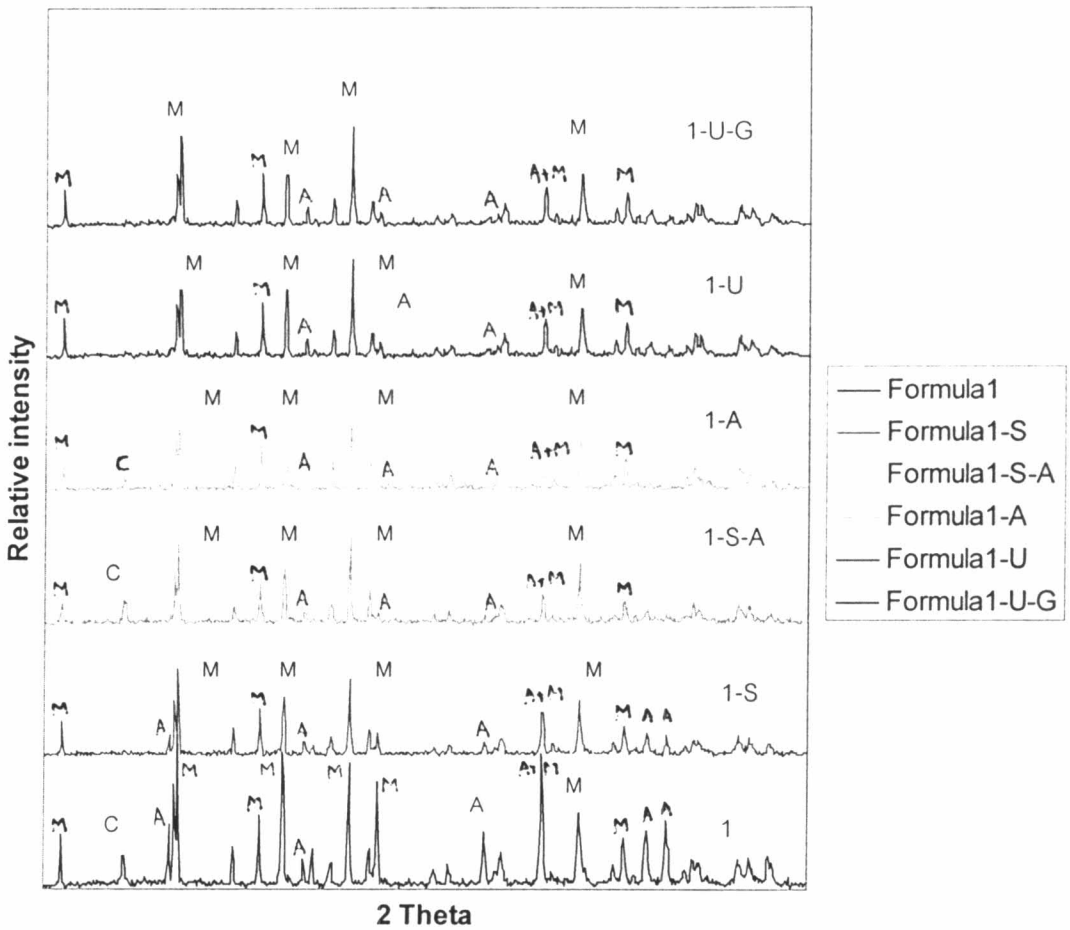

Fig. 4.23 XRD patterns of the specimens with various starting materials sintered at 1400 °C for 5 h.

As shown in Fig. 4.23 the effect of starting materials on the formation of mullite phase, Formula 1 shows higher intensity of mullite phase than the other formulas due to the high purity of silica and alumina but it still shows cristobalite and alumina phases. However, Formula 1-S, 1-U and 1-U-G do not have a cristobalite phase.

It can be concluded that all starting materials for this experiment are capable to produce pure mullite at lower sintering temperature than conventional material. Even the silica from rice husk was used without treatment (SiO_2-U). This is because silica from rice husk has a fine particle size and high specific surface area, then mullitization reaction between silica particles and alumina particles happens at a high rate, so mullitization temperature is reduced.

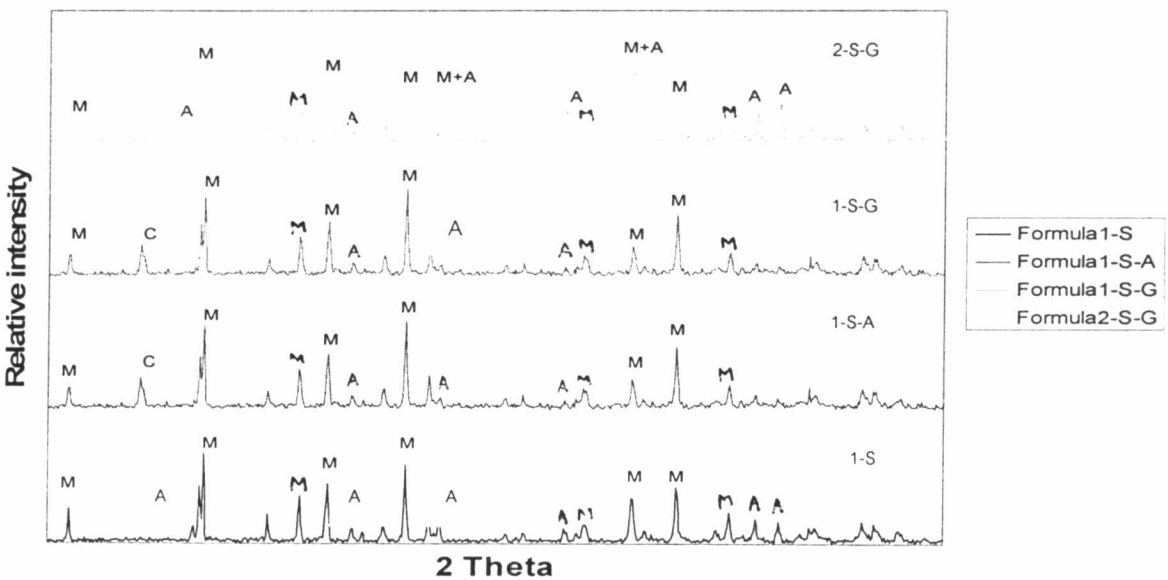

Fig.4.24 XRD patterns of the specimens with various starting materials of alumina, sintered at 1400 °C for 5 h. (same silica source)

Fig.4.24 shows the XRD patterns of the specimens with different sources of alumina. Formula 1-S shows almost mullite phase because it is derived from high purity alumina (A-21).

Formula 1-S-A and 1-S-G are close in the XRD patterns that still have a cristobalite phase. Formula 2-S-G has the lowest mullitization because waste from Al-coating has a low specific surface area and high impurity such as alkali oxide and iron oxide, moreover, waste from Al-coating has high loss on ignition (~ 35%) then it can be used to produce pores between particles of mullite so the reaction sintering is interrupted.

4.2.4.3 The effect of pressing pressure for the phase transformation of mullite.

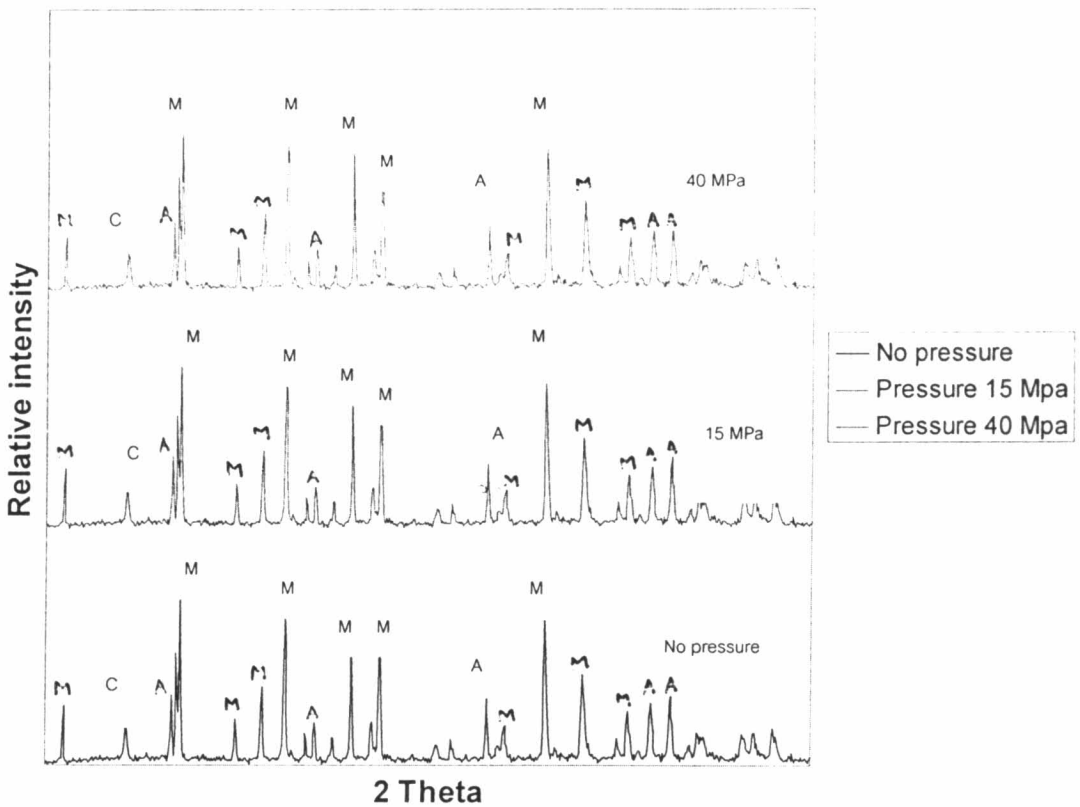

Fig. 4.25 XRD patterns of the specimens under various pressing pressures, sintered at 1400 °C for 5 h (Formula 1)

The pressing pressure for forming the specimens does not relate to the phase transformation of mullite as shown in Fig.4.25. Therefore the process for the synthesis of mullite can be done by calcining the mixture between alumina and silica powders.

4.2.5 Microstructure of sintered specimen examined by scanning electron microscope.

The microstructures of sintered mullite are shown in Fig. 4.26- 4.29. Formula 1-S presents a novel microstructure consisting of fused mullite (2/1 –mullite) which has rod-like grains, whereas Formula 1-A has an acicular grain of higher aspect ratio than Formula1-S.

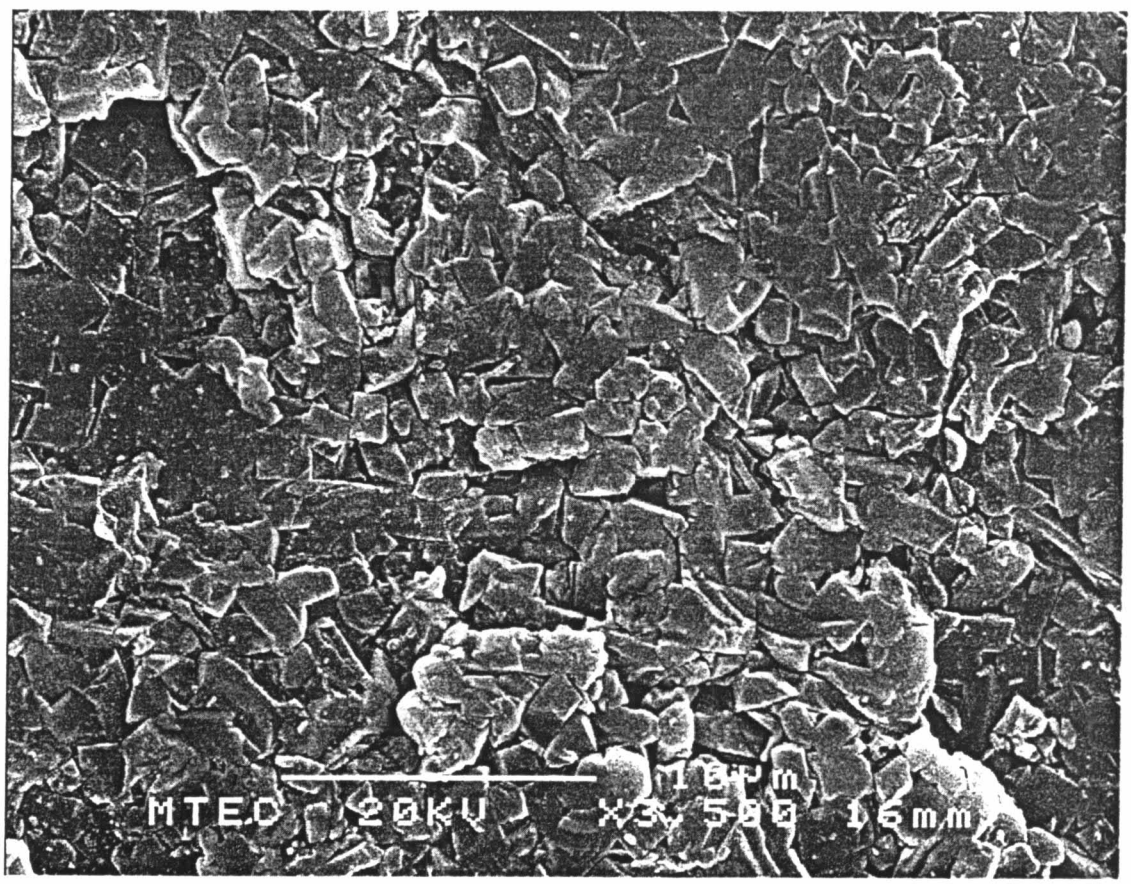

Fig. 4.26 SEM micrograph of specimen Formula 1, sintered at 1700 °C for 3 h.

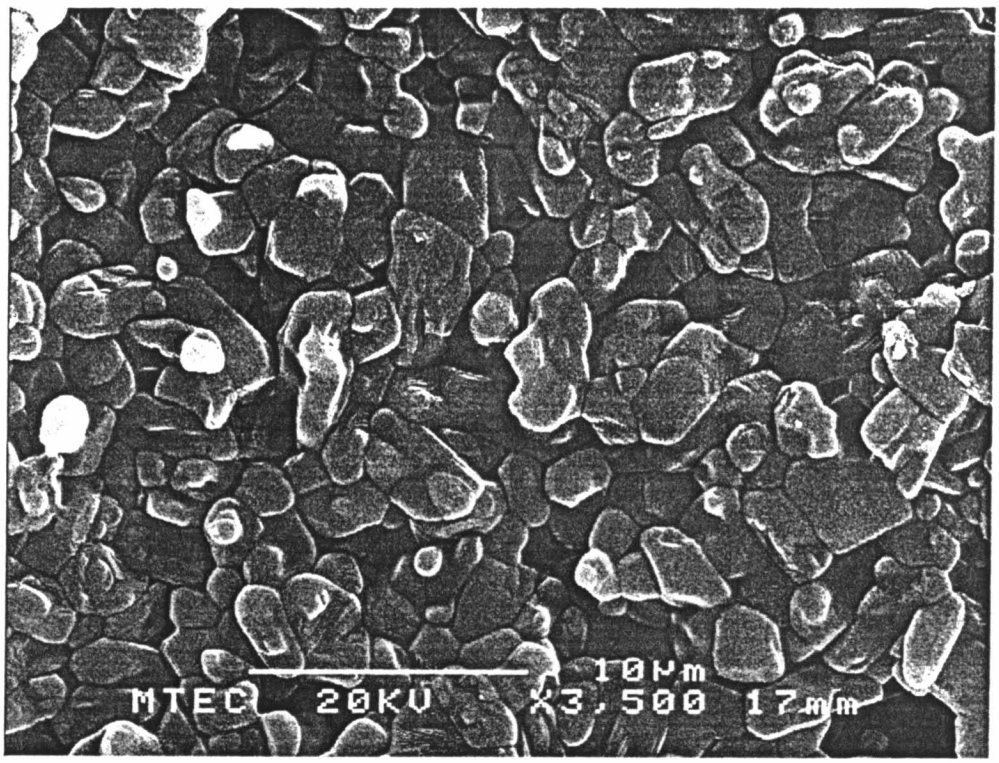

Fig.4.27 SEM micrograph of specimen Formula 1-S, sintered at 1700 °C for 3 h.

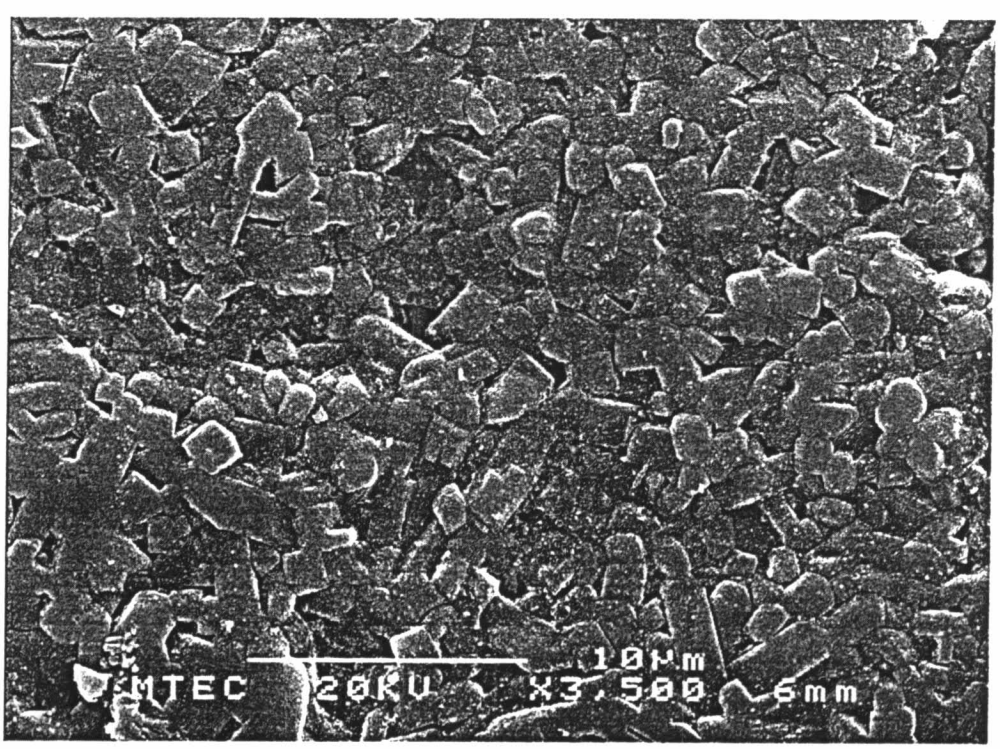

Fig.4.28 SEM micrograph of specimen Formula 1-A, sintered at 1700 °C for 3 h.

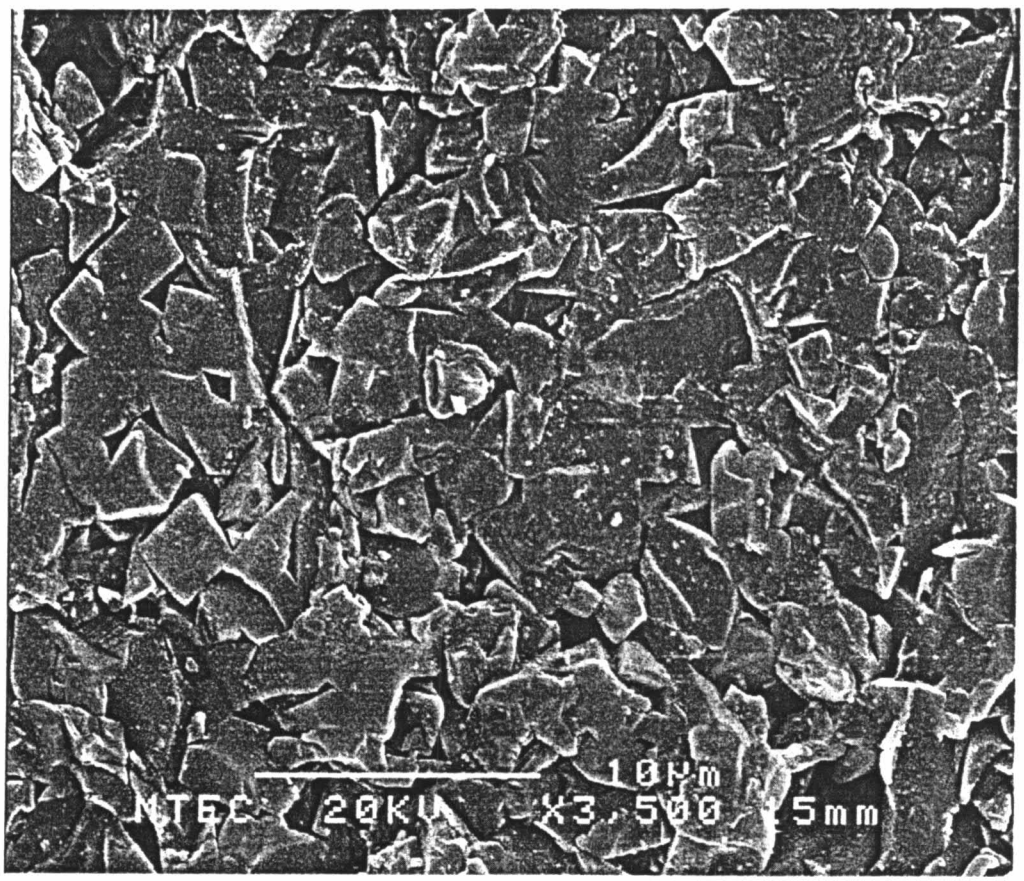

Fig. 4.29 SEM micrograph of specimen Formula 1-S-A, sintered at 1700 °C for 3 h.

The characteristic of the mullite grain in the micrographs is often due to the presence of a glassy phase at grain boundaries which changes the surface energy and therefore the shape of the grain. The effect can also be enhanced by the composition and viscosity of the liquid phase which affects the degree of wetting of the interfaces.

Where there is little glassy phase such as Formula 1, the characteristic morphology would be expected to form their equilibrium shape which is often characteristic and represented by sharp planes and boundaries as shown in Fig. 4.26.[31]

4.2.6 Thermal expansion coefficient (COE) of the specimens.

Table.4.4 Thermal expansion coefficient of the specimen of each formula

Formula	Thermal expansion coefficient (1/°C)
Formula 1	$6.7*10^{-6}$
Formula 1-S	$5.9*10^{-6}$
Formula 1-A	$5.8*10^{-6}$
Formula 1-S-A	$3.6*10^{-6}$
Formula 1-S-G	$4.1*10^{-6}$
Formula 1-U	$5.5*10^{-6}$
Formula 1-U-G	$4.8*10^{-6}$
Formula 2-U-G	$5.7*10^{-6}$
Commercial	$6.8*10^{-6}$

Thermal expansion coefficient is calculated in the temperature range of 20-1000 °C. Normally, the C.O.E of mullite ceramic is ~ $4\text{-}5*10^{-6}$ [2]. Those of formula 1-S-A, 1-S-G and 1-U-G are in the range. However, when compared with commercial mullite, all formulas have lower COE values than commercial mullite from Japan.

In this experiment, due to the limitation of the chamber of dilatometer the length of specimen used for measurement C.O.E is 8 mm. The length is not enough to get high accuracy value. The deviation in the C.O.E values may be caused by the short specimen size, and, of course, the difference in glassy phase contents too.

4.2.7 Bending strength

The results of the bending strength are shown in figure.4.30. It is apparent that the bending strength is related to the bulk density attained in processing. At 1700 °C Formula 1 and 1-S, which used alumina A-21 as raw material, have higher bulk densities than 1-A and 1-S-A that used aluminium oxide from MTEC. The bending strengths of mullite ceramics which used Sumitomo alumina from Japan are higher than those of the other formulas and commercial mullite. It is suggested that alumina A-21 has impurities such as alkali oxide lower than aluminium oxide from MTEC.

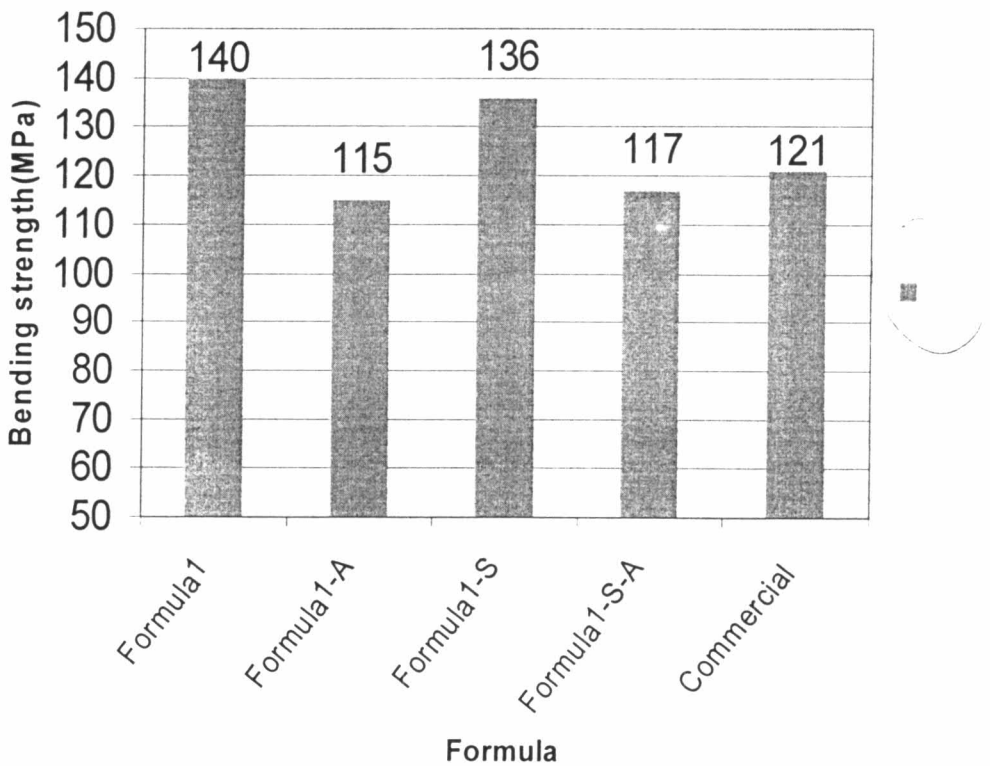

Fig.4.30 Bending strength of mullite ceramics pressed at 40 MPa and sintered at 1700°C.

These impurities generate a glassy phase between the grains of mullite and consequently the mullite has a lower bending strength than mullite without glassy phase.

When the strengths of sintered mullite ceramics were compared with those of previous experiments [22] the strengths of our specimen are lower. It might mainly come from the surface finishing during sample preparation (grinding and polishing).